NASA TECHNICAL
# MEMORANDUM

NASA TM X-2219

NASA TM X-2219

FURTHER STUDIES OF THE EXTRAPOLATION
OF NEAR-FIELD OVERPRESSURE DATA

by Joel P. Mendoza and Raymond M. Hicks

Ames Research Center
Moffett Field, Calif. 94035

1. Report No. NASA TM X-2219	2. Government Accession No.	3. Recipient's Catalog No.
4. Title and Subtitle FURTHER STUDIES OF THE EXTRAPOLATION OF NEAR–FIELD OVERPRESSURE DATA		5. Report Date March 1971
		6. Performing Organization Code
7. Author(s) Joel P. Mendoza and Raymond M. Hicks		8. Performing Organization Report No. A-3716
9. Performing Organization Name and Address NASA Ames Research Center Moffett Field, Calif., 94035		10. Work Unit No. 720-01-10-02-00-21
		11. Contract or Grant No.
12. Sponsoring Agency Name and Address National Aeronautics and Space Administration Washington, D. C. 20546		13. Type of Report and Period Covered Technical Memorandum
		14. Sponsoring Agency Code

15. Supplementary Notes

16. Abstract

    The technique of extrapolating measured near-field overpressure data to any larger altitude has been applied to wind-tunnel overpressure data for a wide variety of wing-body combinations. A compilation of measured and extrapolated overpressure data is presented here in an effort to show the range of configurations for which the extrapolation technique is applicable. Included are simple shapes, such as cone-cylinder and unswept wing-alone models, as well as complete airplane configurations (e.g., X-15 and supersonic transport models). The range of test Mach numbers was 1.41 to 3.0, while the altitude to model length ratio varied from 1 to 20. Except for the case of a high aspect ratio wing-alone model, the extrapolation procedure was shown to give almost perfect agreement with experimental measurement; even for the high aspect ratio wing alone, the agreement was adequate. A method for determining the validity of the extrapolation is discussed.

17. Key Words (Suggested by Author(s)) Sonic boom Near field pressure signature Far field pressure signature Flow field pressure distribution Overpressure characteristics Near field overpressure data	18. Distribution Statement Unclassified — Unlimited		
19. Security Classif. (of this report) Unclassified	20. Security Classif. (of this page) Unclassified	21. No. of Pages 35	22. Price* $3.00

NOTATION

C_L lift coefficient

h   model altitude

K_r reflection factor

l reference length of model

M   Mach number

p   reference pressure

Δp difference between local and free-stream static pressures

Δx distance measured parallel to longitudinal axis of model from point in undisturbed stream to point on pressure signature

FURTHER STUDIES OF THE EXTRAPOLATION OF

NEAR–FIELD OVERPRESSURE DATA

Joel P. Mendoza and Raymond M. Hicks

Ames Research Center

SUMMARY

The technique of extrapolating measured near-field overpressure data to any larger altitude has been applied to wind-tunnel overpressure data for a wide variety of wing-body combinations. A compilation of measured and extrapolated overpressure data is presented here in an effort to show the range of configurations for which the extrapolation technique is applicable. Included are simple shapes, such as cone-cylinder and unswept wing-alone models, as well as complete airplane configurations (e.g., X-15 and supersonic transport models). The range of test Mach numbers was 1.41 to 3.0, while the altitude to model length ratio varied from 1 to 20. Except for the case of a high aspect ratio wing-alone model, the extrapolation procedure was shown to give almost perfect agreement with experimental measurement; even for the high aspect ratio wing alone, the agreement was adequate. A method for determining the validity of the extrapolation is discussed.

INTRODUCTION

In 1967 a procedure was developed at Ames Research Center that permitted the extrapolation of near-field pressure signatures for arbitrary airplane configurations to any greater altitude (ref. 1). Although the technique has been used by several investigators with considerable success, only one additional report on the use of the procedure has appeared in the literature (ref. 2). Because of this lack of experimental or theoretical verification of the extrapolation technique, some theoreticians have expressed doubt as to the validity of the method for extrapolating near-field pressure signatures for certain types of configurations (e.g., configurations exhibiting large regions of two-dimensional flow, such as high aspect ratio wings, or configurations with vertically displaced lifting elements resulting in considerable asymmetry of the flow field). As a consequence, a study was made of the extrapolations of pressure signature data of configurations having some of the geometric properties that raised doubts about the technique. This report contains a compilation of the results of that study.

MODELS, APPARATUS, AND TESTS

The pressure signatures of several different models were measured in the Ames 9- by 7-Foot and 8- by 7-Foot wind Tunnels. A typical arrangement of the test apparatus with a model is shown in figure 1. The model flow-field pressures were measured using a system consisting of a differential pressure transducer connected to two pressure probes mounted on the wall of the wind tunnel.

Each probe was a slender cone with a total angle of 2°. Four pressure orifices were drilled at 90° intervals around the circumference of each probe. The orifices of the reference probe were in a plane normal to the direction of the flow. The plane containing the orifices of the overpressure probe was tangent to the Mach cone originating from the nose of the model. The normal force of the models was measured by an internal strain gage balance.

The study also included pressure signatures from two different sonic boom tests conducted in the Langley 4- by 4-Foot Wind Tunnel. One test, reported in reference 3, utilized a boundary-layer bypass plate for the measurements of the flow field pressures of two wing-alone models. The plate was considered to have a reflection factor of 2.0. The test was conducted at a Mach number of 2.01.

The other test consisted of measurements of pressure signatures for two supersonic transport models reported in reference 4. For this test the pressures were measured with conical probes at Mach numbers of 1.41 and 2.01.

The first four models examined in this report are simple geometric shapes. Models I(a) and I(b), shown in figure 2, are cone-cylinders. Although differing in size, both models have identical fineness ratios and angles. The pressure signature of the larger cone-cylinder model (model I(a)) was measured at an altitude of 86.0 in., which was equivalent to 10.0 cone lengths. To obtain measurements of the overpressure characteristics at 20.0 lengths, model I(b) (one-half the size of model I(a)) was also tested at an altitude of 86.0 in. Model II, shown in figure 3, is a wing with a rectangular planform, an aspect ratio of 0.5, and a biconvex wing section. Model III, shown in figure 4, is a rectangular wing with an aspect ratio of 2 and a wedge airfoil section.

The remainder of the models examined herein were more complex. The wing-body models (IV and V) shown in figures 5 and 6 were constructed of mild steel with the wings and body as an integral unit. These two models were designed to be mounted on a 0.30-in. diameter internal strain gage balance. Model VI (fig. 7) is a 0.0107 scale model of the X-15 airplane and was a one-piece casting of beryllium-copper. Models VII through IX, shown in figures 8 through 10, were constructed with the wings and body as an integral unit. All three models were constructed of 17-4 PH stainless steel.

The Langley supersonic transport models, designated X and XI, are shown in figure 11. Model X is the basic model while model XI is modified to produce a flat top pressure signature. The models are fully described in reference 4.

The models, apparatus, and test conditions were varied somewhat in each wind tunnel; the various test parameters are given in table 1.

RESULTS AND DISCUSSION

Flow-field pressure measurements from several different wind-tunnel tests were used for investigating the effects of configuration, Mach number, and altitude on the technique of extrapolating measured near-field pressures to larger altitudes. This investigation included measured pressure signatures of two rectangular wings from reference 3 and measured pressure signatures from models of a supersonic transport from reference 4.

2

Figures 12 through 22 show measured and extrapolated pressure signatures of the various test models. Flow-field pressures measured at the smaller altitudes were extrapolated and compared with the measured pressure signatures at the larger altitudes where generally good agreement was noted.

Models I(a) and I(b)

Figure 12 shows the pressure signatures of model I, the cone-cylinder, at the Mach number of 1.68. Since the extrapolation technique is based on the expressions given by Whitham, formulated from axisymmetric considerations, the excellent agreement noted between the measured and extrapolated flow-field pressure distributions at an altitude of 20 cone lengths is not considered unusual.

Models II and III

The pressure signatures of models II and III, at a Mach number of 2.01, are shown in figures 13 and 14, respectively. The geometrical and flow-field characteristics of these two models provide interesting contrasts. Note that an extrapolation of the measured flow-field pressure distributions of model II from an altitude of 1 chord length produced good agreement with the measured pressures at an altitude of 8 chord lengths. For model III the extrapolation from 2 to 16 chord lengths produced good agreement with the maximum overpressure, whereas the extrapolated expansion slope was somewhat less than experiment. This is not too surprising since from theoretical considerations the flow field for this model must exhibit more two-dimensional characteristics than model II. Although the extrapolation (fig. 14) from 2 to 16 chord lengths is not as good as the other extrapolations shown in this report, it is better than might be expected for this model.

In the case of model II the curved surface of the wing produces expansion wavelets that interact immediately with the two-dimensional oblique shock attached to the wing leading edge. This interaction reduces the shock strength, causing the angle of the shock wave to turn in the direction approaching the free-stream Mach angle. Because of the low aspect ratio of model II, three-dimensional effects develop quickly, so that quite close to the wing the flow field becomes essentially axisymmetric in each azimuthal plane. In contrast to the curved surfaces of model II, model III features planar surfaces and a higher aspect ratio. The two-dimensional oblique shock attached to the wing leading edge remains undisturbed over a relatively large distance from the chord plane of the wing. Expansion wavelets emanating from the wing trailing edge will not interact with the planar shock wave until an altitude of approximately 6 chord lengths is reached. At this point, as in the case of model II, the shock strength and the shock wave angle are reduced. At an altitude of approximately 8 chord lengths the two-dimensional flow characteristics become negligible. Beyond this altitude the flow behaves as if it were axisymmetric in each azimuthal plane.

To assure the validity of the extrapolated results, the region of applicability of the extrapolation technique must first be established. While the extrapolation technique is recognized as a development of the form of Whitham's equation, which is valid only in the region of the flow field far from the body, extrapolated results shown herein and in references 1 and 2 indicate that the extrapolation technique may not be completely restricted by the assumption of large altitude. It is expected, however, that a point in the flow field near the body may be reached where the flow

3

cannot be regarded as axisymmetric, and extrapolations of overpressure data measured at this point will not accurately predict the overpressure characteristics at larger altitudes. The extrapolation of overpressure data from 2 chord lengths to 16 chord lengths in figure 14 illustrates this effect. However, it will be shown in the following section that the extrapolation technique when applied to realistic aircraft configurations will accurately define the overpressure characteristics at large altitudes using data measured at 1 body length.

Models IV and V

The overpressure characteristics of models IV and V at a Mach number of 1.68 and at two lift coefficients are shown in figures 15 and 16, respectively. The test altitudes ranged from 1 to 11.3 body lengths. Although the pressure measurements made at an altitude of 1 body length might be expected to be too close to the body for application of the extrapolation technique, the extrapolations proved quite satisfactory. The extrapolations of the overpressure characteristics from an altitude of 1 to 7.25 and 11.3 body lengths did not exhibit the large discrepancies one might expect in the comparisons with the measured pressure signatures at the larger altitudes. The existence of far-field characteristics of the pressure signature at a lift coefficient of 0.277 shown in figure 15 is accurately predicted at the altitudes of 7.25 and 11.3 body lengths. The extrapolated pressure signature for model V (fig. 16) at an altitude of 11.3 body lengths and a lift coefficient of 0.278 distinctly shows the existence of a secondary shock that is not detected in the measured pressure signature. It is believed that a closer spacing of the data points in that region might indicate the existence of the shock. It can be seen that for these two models the region of applicability extends into 1 body length.

Models VI – IX

Figures 17 through 20 illustrate further that overpressure characteristics of configurations with greatly differing planforms can be accurately predicted by the extrapolation technique. Figures 17(a) and 17(b) show the measured and extrapolated pressure signatures of model VI a 0.0107 scale model of the X-15 airplane is complete with empennage, canopy, and side fairings. The flow-field pressure distributions of model VII featuring a blunt nose (the cross-sectional area of the nose is proportional to $x^{1/2}$) at a Mach number of 1.68 are shown in figure 18. Excellent correlations between measured and extrapolated pressure signatures for model VIII which was considered to produce large flow-field asymmetry are shown in figures 19(a) and 19(b) at the Mach numbers of 1.68 and 2.70, respectively.

Models X and XI

Models X and XI are the basic and modified configurations, respectively, of a supersonic transport design; both are complete with empennage and engine pods. The cross-sectional area distributions of the two models differ only in the region of the nose. The design considerations are discussed in detail in reference 4. Pressure signatures measured at the lowest test altitude were extrapolated and compared to the pressure signatures measured at the largest test altitude where good correlation is noted in all cases. Figure 21 shows the measured and extrapolated pressure signatures of model X at Mach numbers of 1.41 and 2.01. The measured and extrapolated overpressure characteristics of model XI are given in figure 22.

4

Models IV and V Extrapolated to Flight Altitudes

Figures 23 and 24 show the overpressure characteristics of models IV and V, respectively, at the altitudes of 1 and 11.3 body lengths, and the extrapolation of the flow field pressure distributions of each model from 1 body length to altitudes of 11.3 and 130 body lengths. At an altitude of 11.3 body lengths the extrapolated pressure signature is seen to agree quite closely with the measured pressure signature. Although the peak pressures are slightly different, the impulse areas appear to be approximately equal. The small differences noted at an altitude of 11.3 body lengths appear to be early indications of large differences that would exist at flight altitudes. To test this contention, the measured overpressure characteristics at an altitude of 11.3 body lengths were extrapolated to an altitude of 130 body lengths. These extrapolated results were compared to the data previously extrapolated from an altitude of 1 to 130 body lengths, and it is observed that for both models the extrapolations agree quite closely. These agreements are attributed largely to the fact that the impulse areas are approximately equal at the altitude of 11.3 body lengths.

CONCLUDING REMARKS

Overpressure characteristics for a number of different test models measured at small altitudes have been extrapolated and compared to overpressure characteristics measured at larger altitudes. For airplane configurations the extrapolation technique, using overpressure data measured at altitudes as low as 1 body length, was shown to predict the overpressure characteristics accurately at larger altitudes. The assumption of large altitude that led to the development of the widely used form of Whitham's theory on which the extrapolation technique is based does not appear to place a strong altitude restriction on the use of the extrapolation technique.

Ames Research Center
    National Aeronautics and Space Administration
        Moffett Field, Calif., 94035, Sept. 22, 1970

REFERENCES

1. Hicks, Raymond M.; and Mendoza, Joel P.: Prediction of Aircraft Sonic Boom Characteristics From Experimental Near Field Results. NASA TM X–1477, 1967.

2. Morris, Odell A.; Lamb, Milton; and Carlson, Harry W.: Sonic-Boom Characteristics in the Extreme Near Field of a Complex Airplane Model at Numbers of 1.5, 1.8, and 2.5. NASA TN D–5755, 1970.

3. Carlson, Harry W.: An Investigation of Some Aspects of the Sonic Boom by Means of Wind-Tunnel Measurements of Pressures About Several Bodies at a Mach Number of 2.01. NASA TN D–161, 1959.

4. Carlson, Harry W.; McLean, F. Edward; and Shrout, Barret L.: A Wind-Tunnel Study of Sonic Boom Characterisitics for Basic and Modified Models of a Supersonic Transport Configuration. NASA TM X–1236, 1966.

TABLE 1.— TEST PARAMETERS

Model	Test Mach number	Stagnation pressure, Hg	Test facility
I(a)	1.68	30.0	Ames 9- by 7-foot
I(b)	1.68	30.0	
II	2.01	- - -	Langley 4- by 4-foot
III	2.01	- - -	
IV	1.68	20.0	Ames 9- by 7-foot
V	1.68	20.0	
VI	2.0	30.0	
	3.0	30.0	Ames 8- by 7-foot
VII	1.68	20.0	Ames 9- by 7-foot
	2.70	20.0	Ames 8- by 7-foot
VIII	1.68	20.0	Ames 9- by 7-foot
	2.70	20.0	Ames 8- by 7-foot
IX	2.70	20.0	
X	1.41	21.0	Langley 4- by 4-foot
	2.01	21.0	
XI	1.41	21.0	
	2.01	21.0	
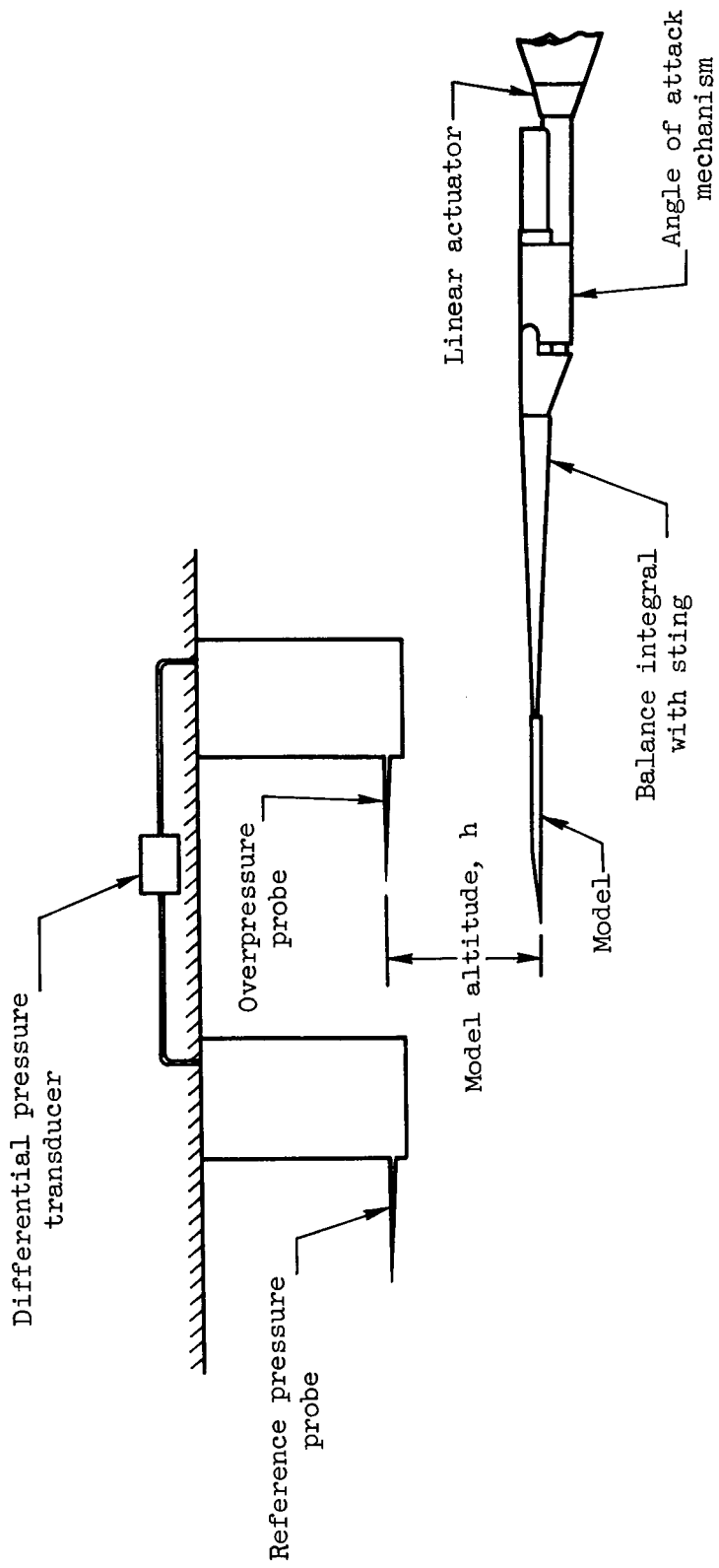
Figure 1.- Wind-tunnel apparatus.

Note: All dimensions are in inches

6.48°

8.60

1(a)

6.48°

4.30

1(b)
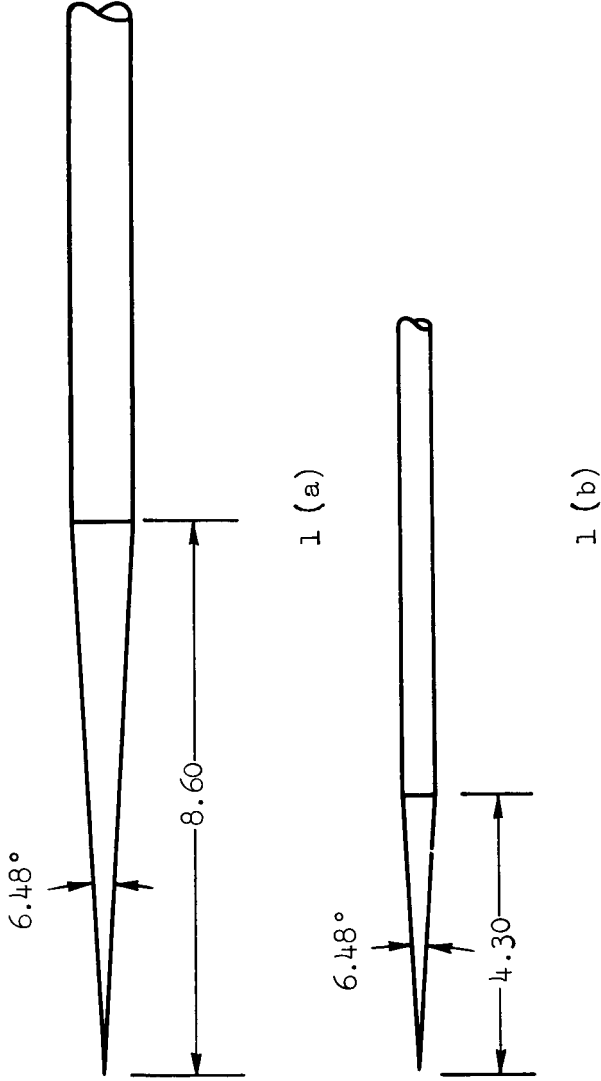
Figure 2.- Models I(a), I(b), (cone-cylinder models).
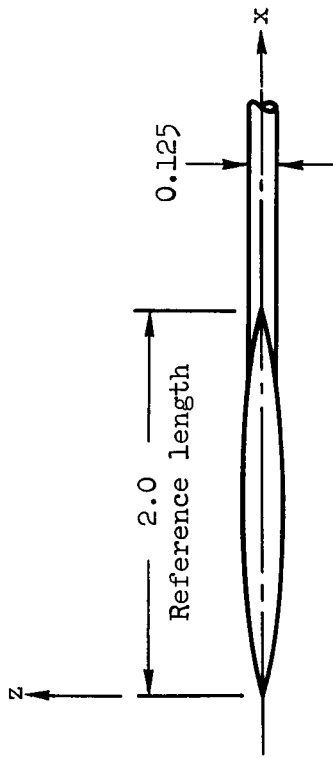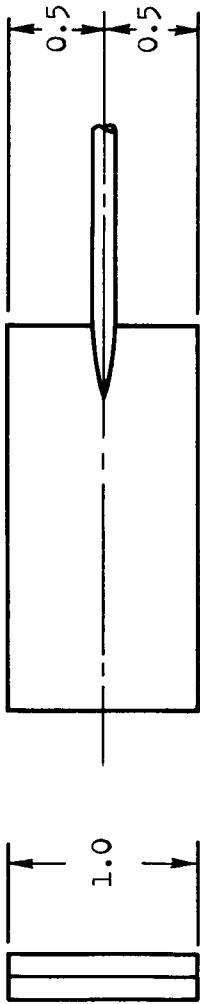
Note: All dimensions are in inches

Thickness distribution is given by $z = \dfrac{\pi}{12.5}\left(x - \dfrac{x^2}{2}\right)$

Figure 3.- Model II, aspect ratio = 0.5.
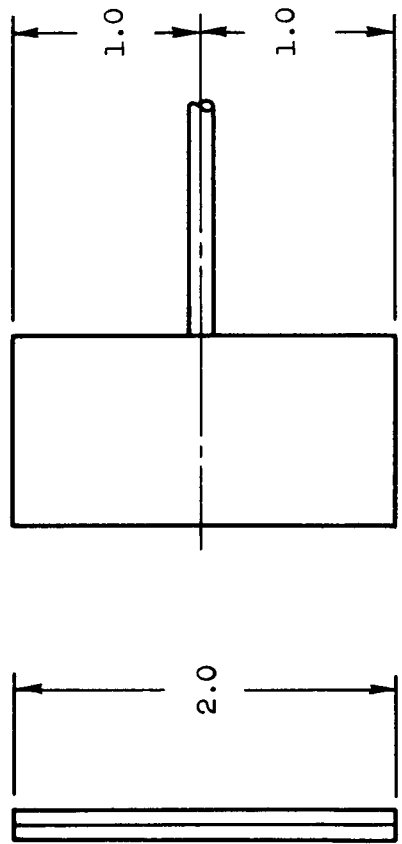
Note: All dimensions are in inches
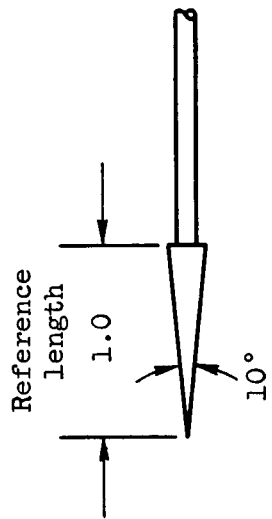
Figure 4.- Model III, aspect ratio = 2.0.

Nose radius is given by
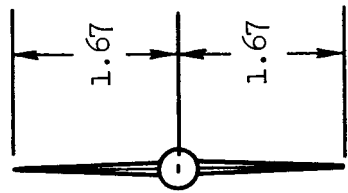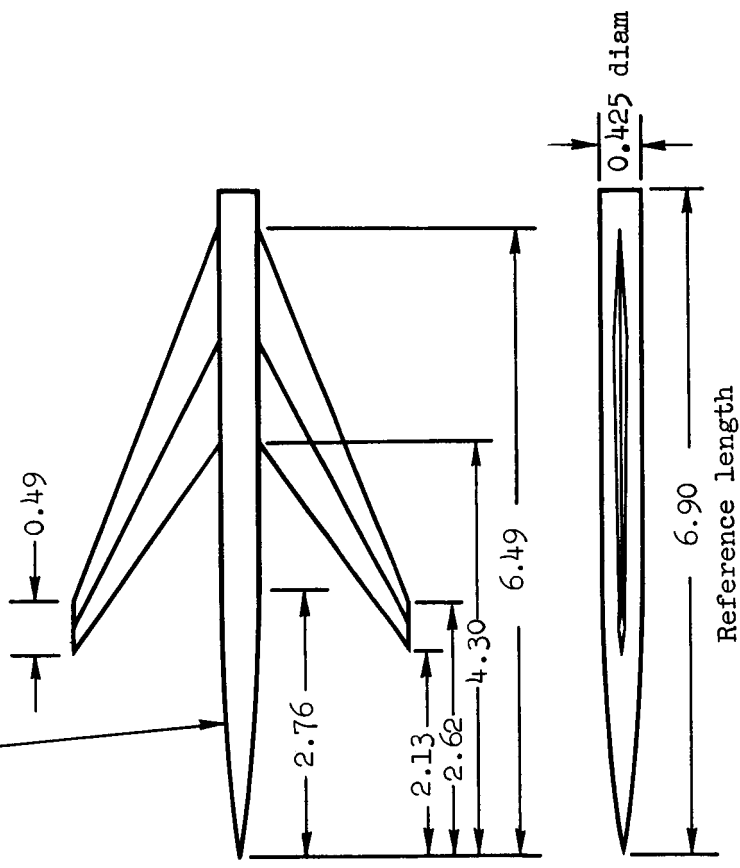
$$r = 0.2125 - 0.027895 (x - 2.76)^2 \qquad 0 \leq x \leq 2.76$$

0.49

2.76

2.13

2.62

4.30

6.49

0.425 diam

6.90

Reference length

1.67

1.67

Figure 5.- Model IV.

Note: All dimensions are in inches

11

Nose radius is given by
$r = 0.2125 - 0.027895 (x - 2.76)^2$ $0 \leq x \leq 2.76$

2.76

4.45

4.71

5.79

6.05

1.67

1.67

0.425 diam

6.90

Reference length
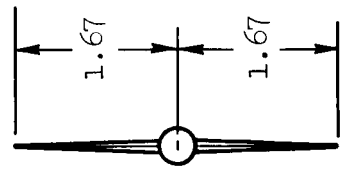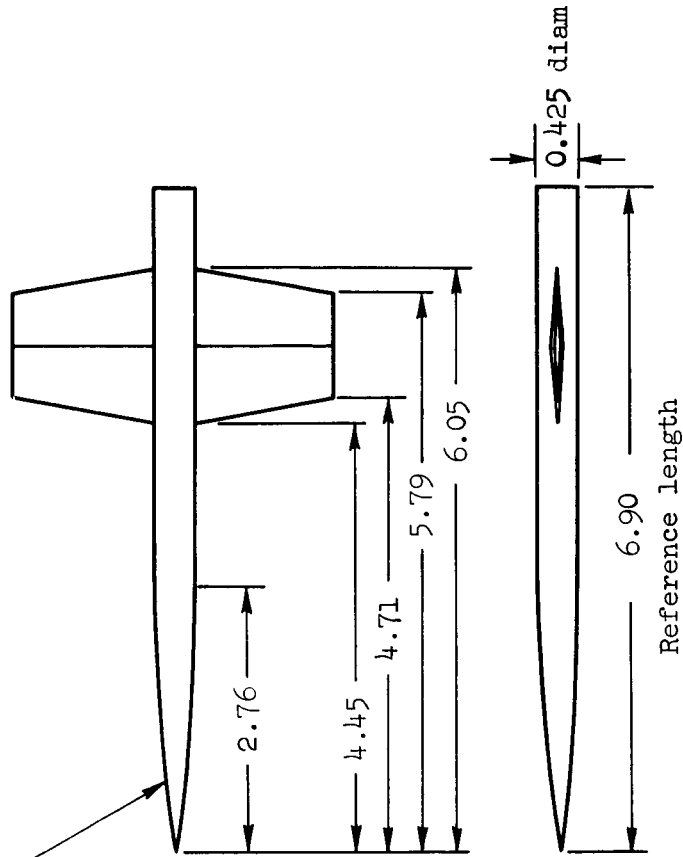
Note: All dimensions
are in inches

Figure 6.- Model V.

4.80
Reference length

1.05 — 1.05
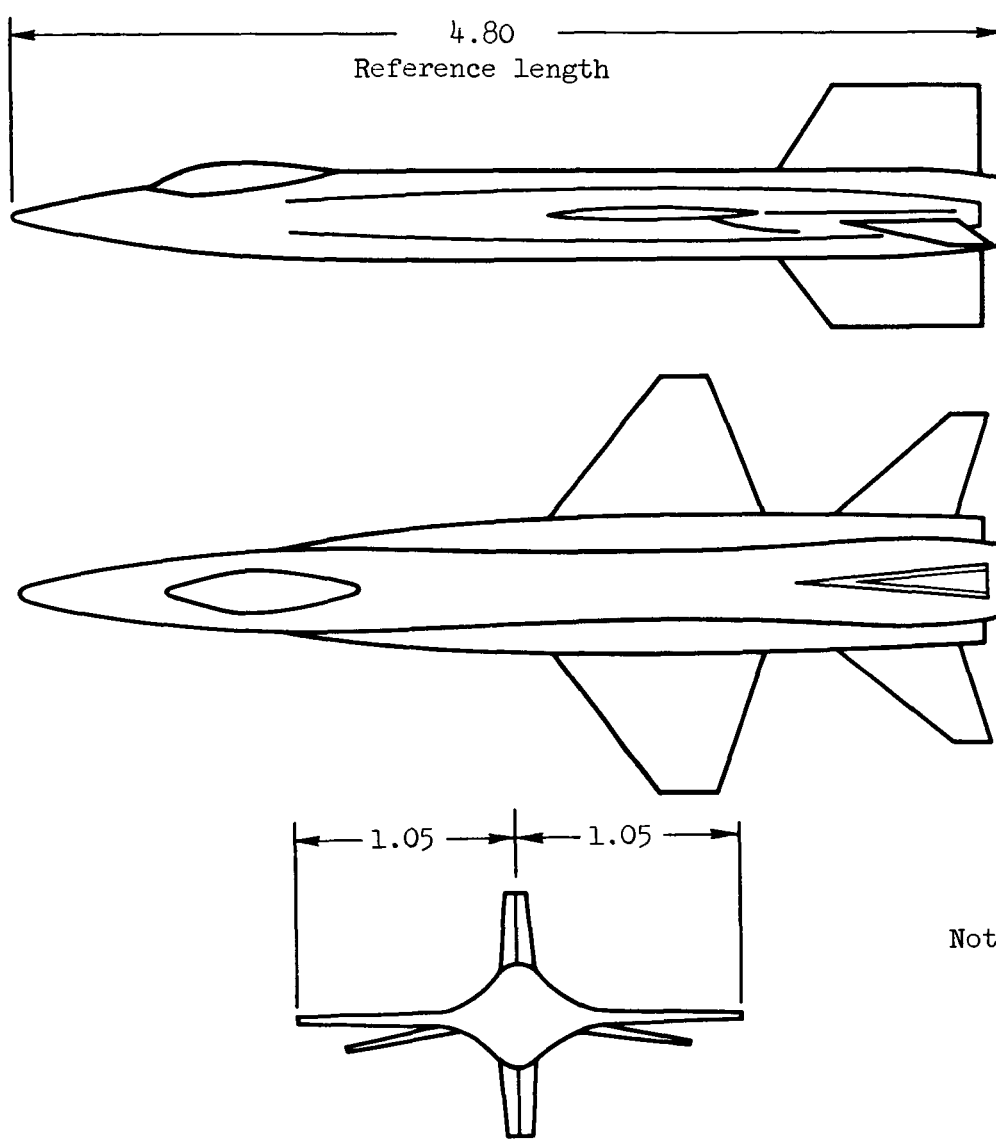
Note: All dimensions
are in inches

Figure 7.- A 0.0107 scale model of the X-15 airplane (model VI).

Nose radius is given by

$r = 0.164866x^{\frac{1}{4}}$ $0 \le x \le 2.76$

0.74

0.74

0.425 diam

1.67

2.76

5.75

8.50

9.00

10.00

Reference length

1.75

1.75

10°

Note: All dimensions
are in inches
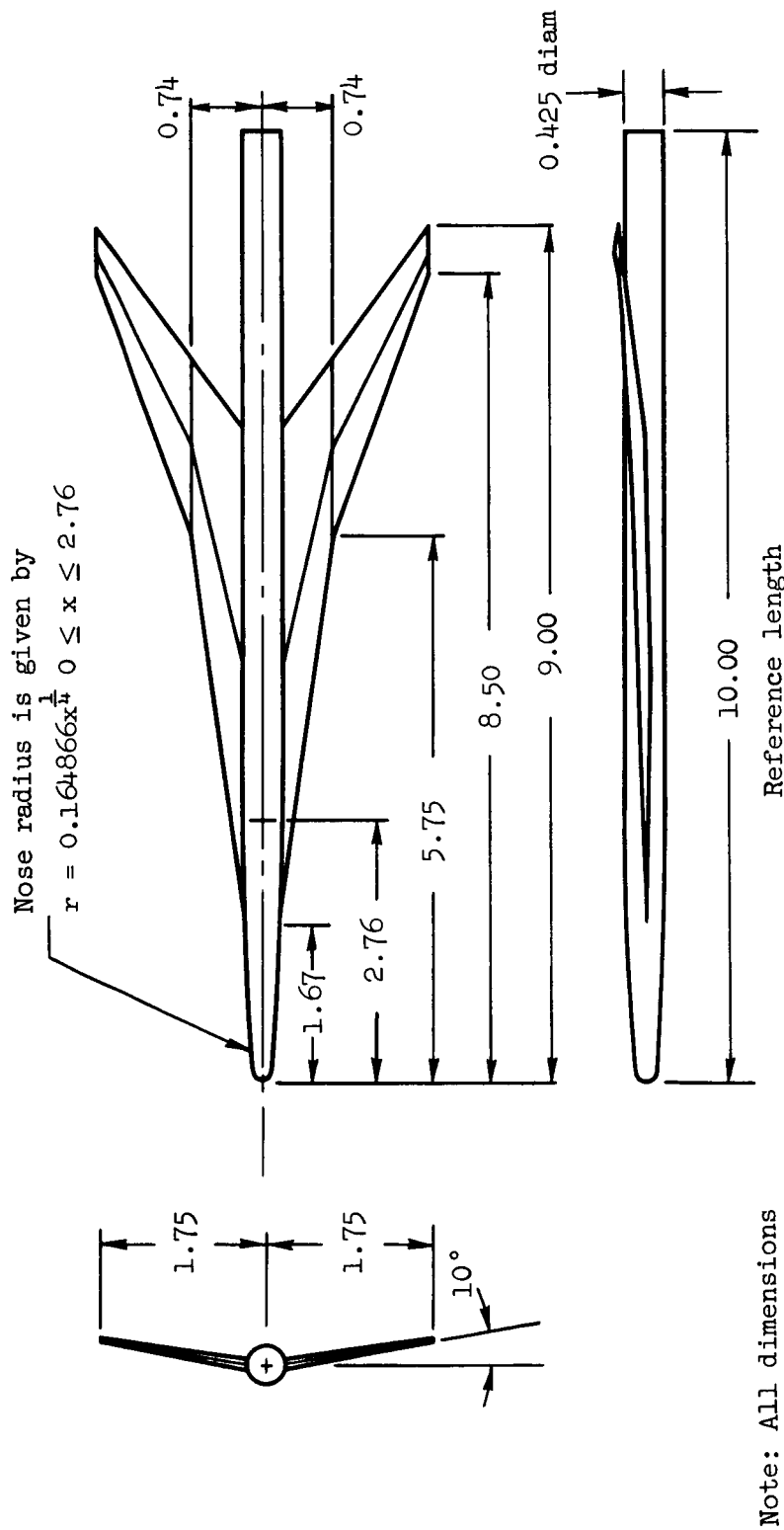
Figure 8.- Model VII.

Note: All dimensions are in inches

10.84
Reference length

83°

69°
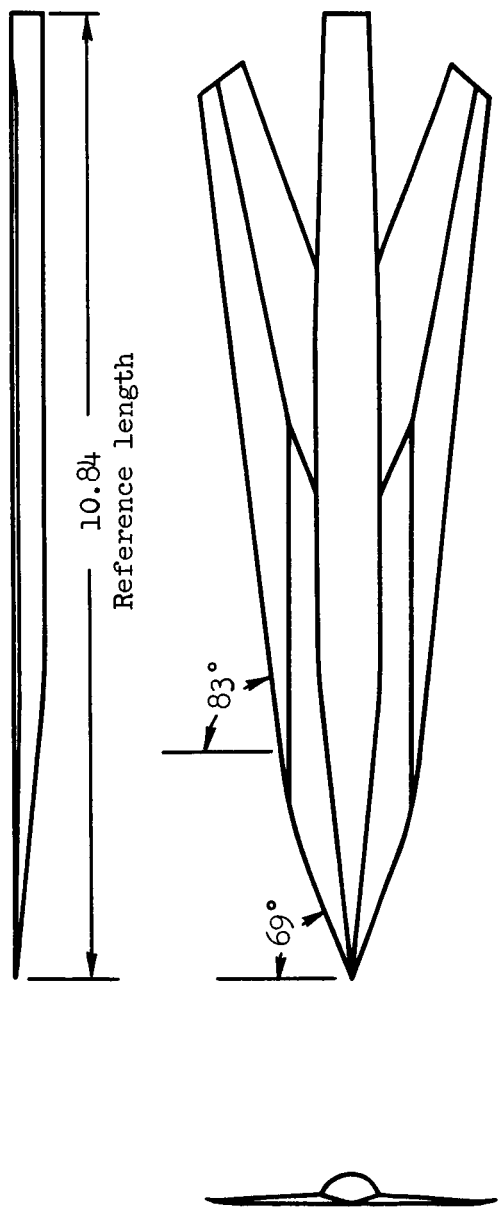
Figure 9.- Model VIII.
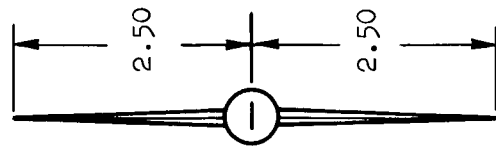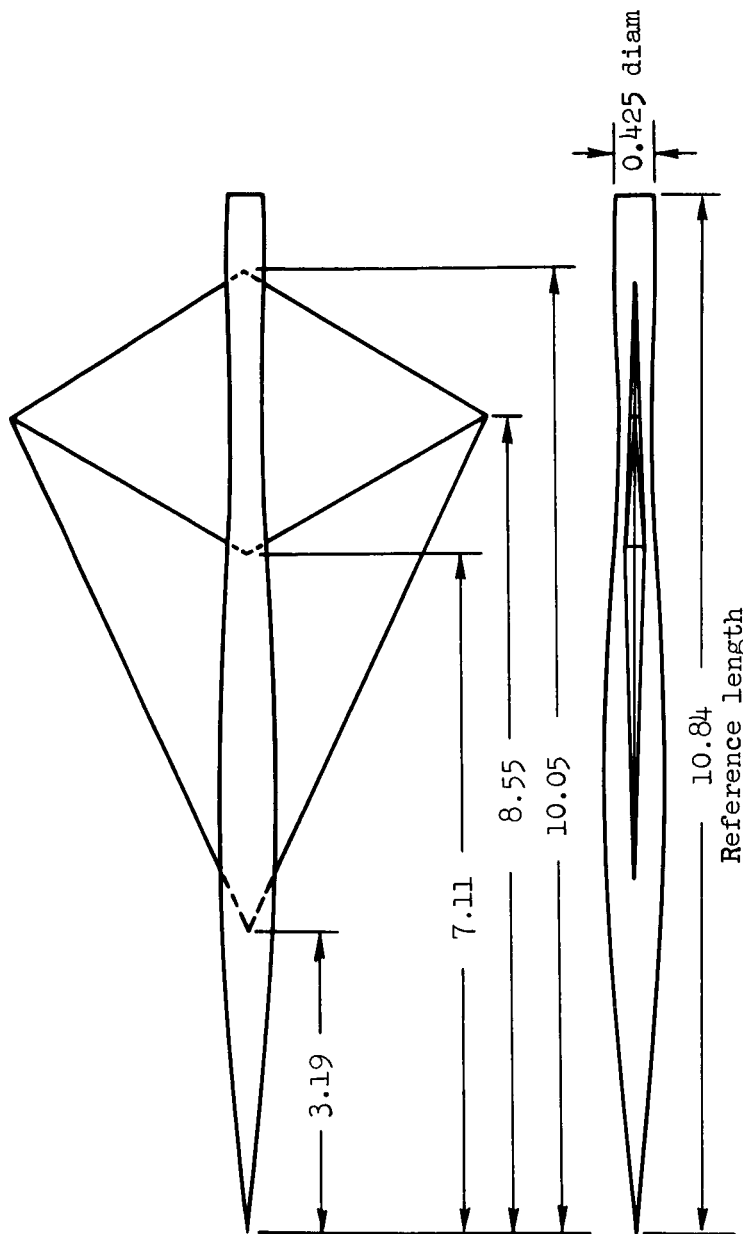
Figure 10.- Model IX.

Note: All dimensions are in inches
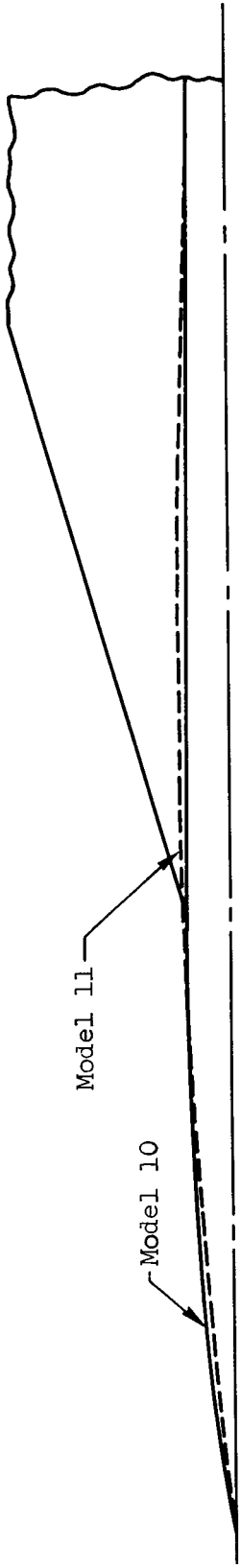
Detailed view showing the geometrical differences between models 10 and 11.

Model 11

Model 10

Note: All dimensions
are in inches

3.93

Reference length
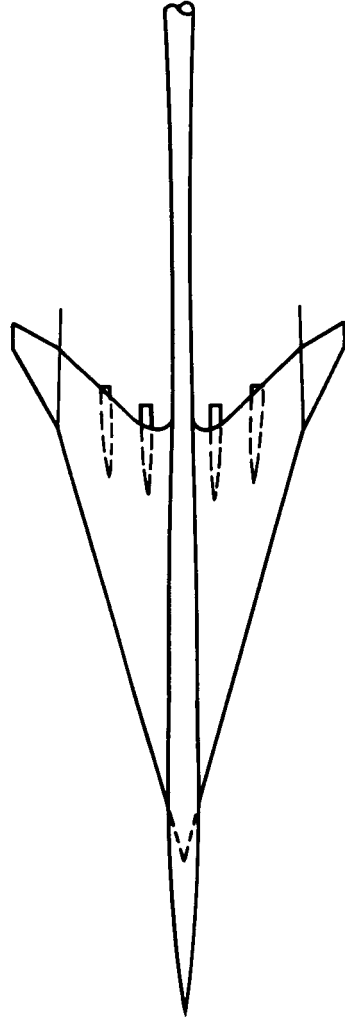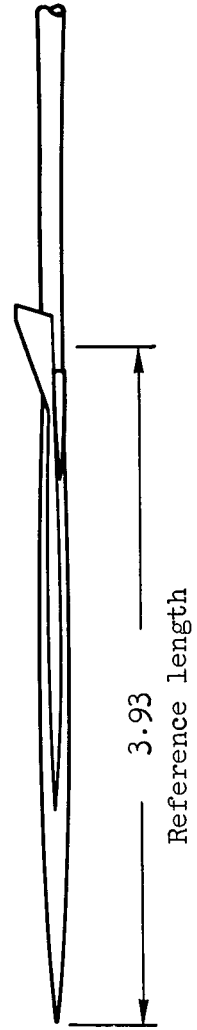
Figure 11.- Models X and XI.
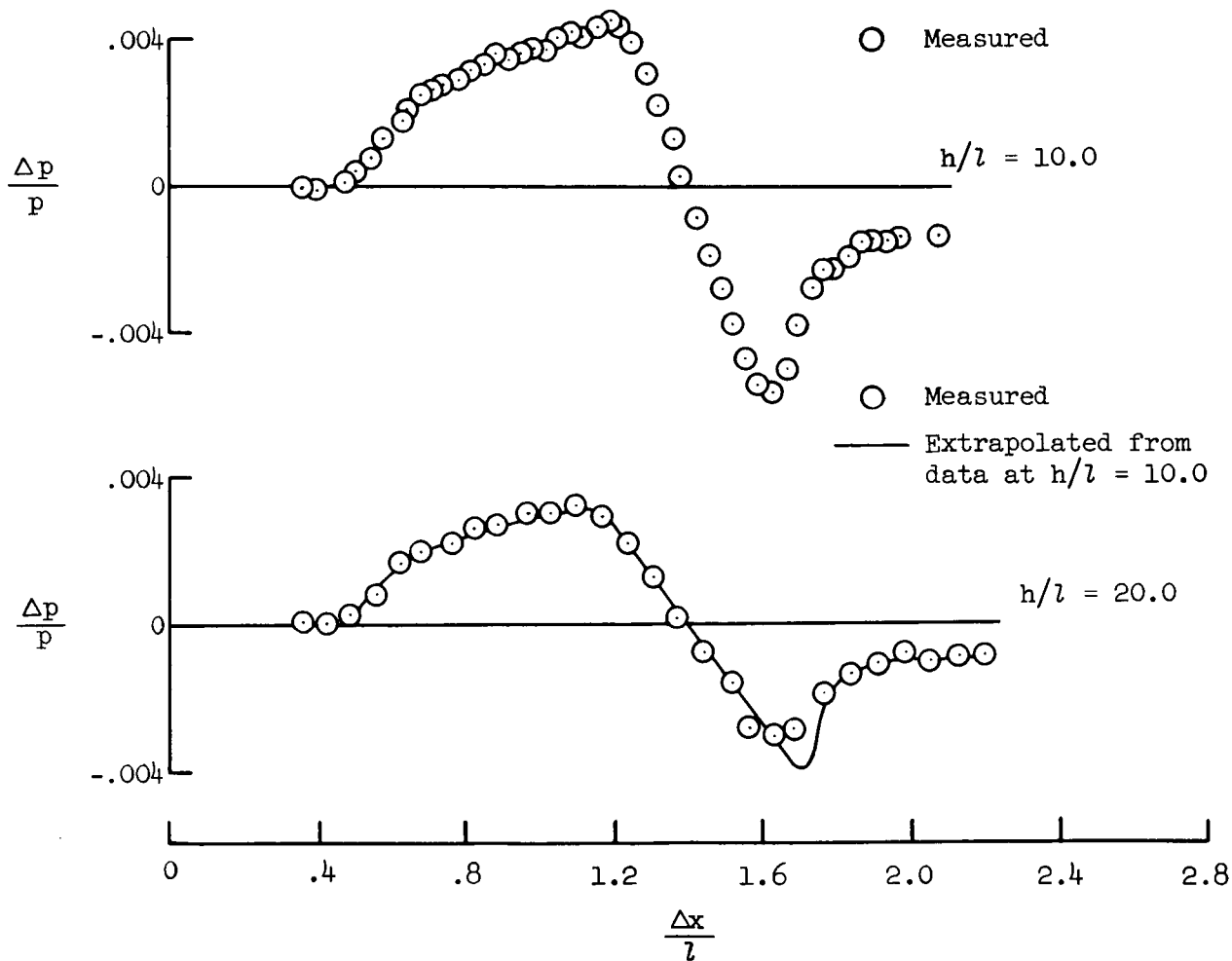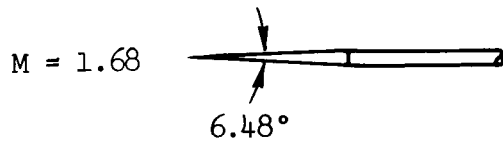
Figure 12.- Flow-field pressures of model I.
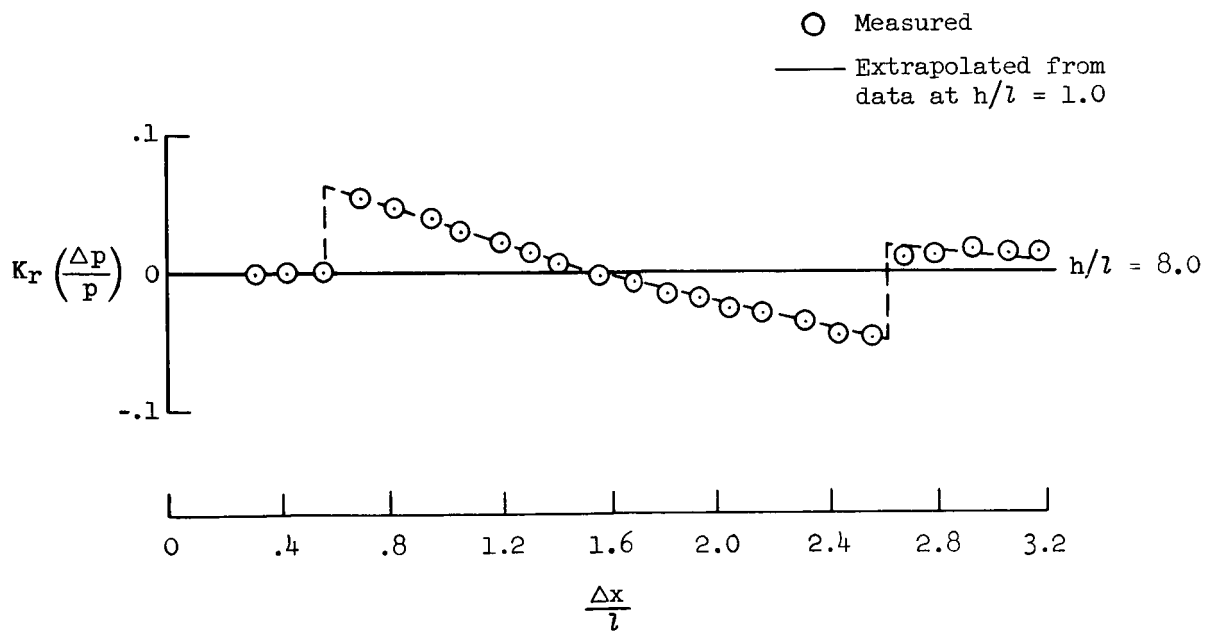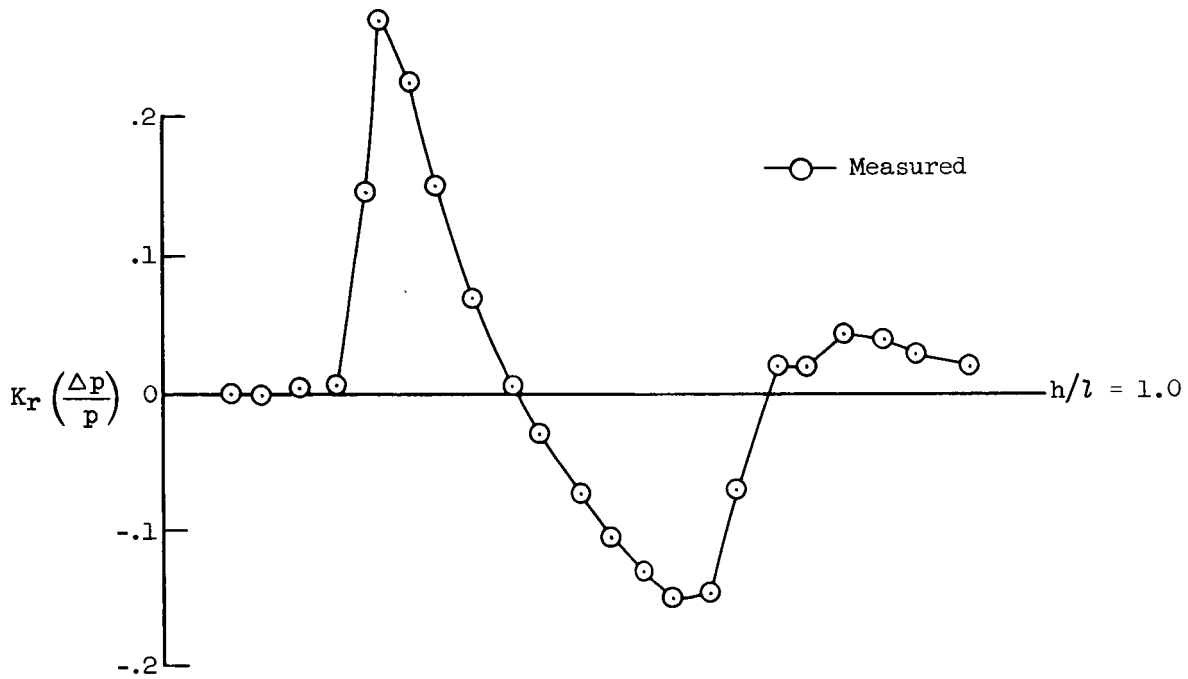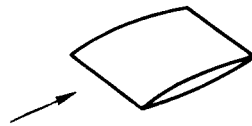
Figure 13.- Flow-field pressures of model II measured on a boundary layer bypass plate at $M = 2.01$, $K_r = 2.0$.
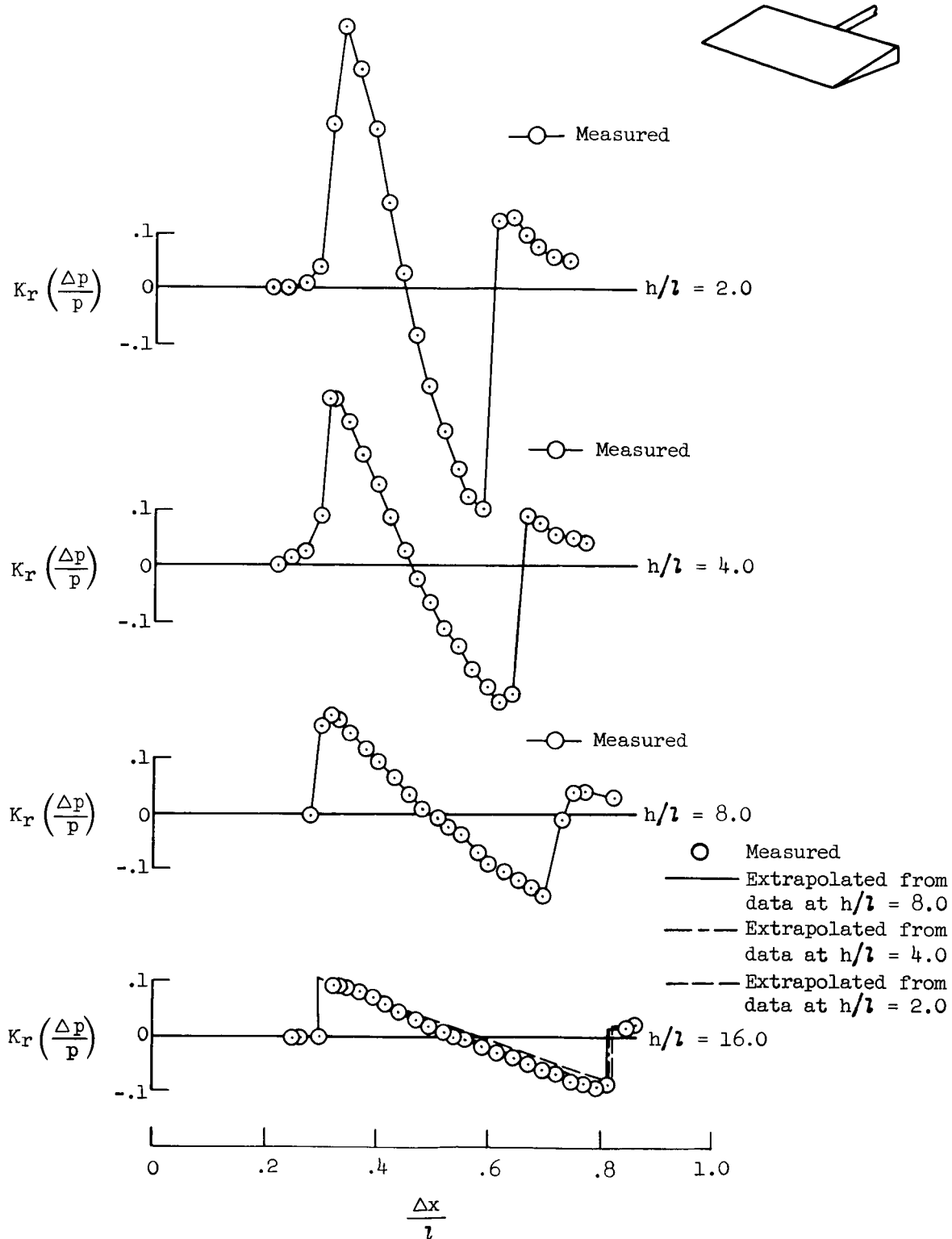
Figure 14.- Flow-field pressures of model III measured on a boundary layer bypass plate at $M = 2.01$; $K_r = 2.0$.
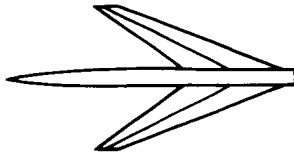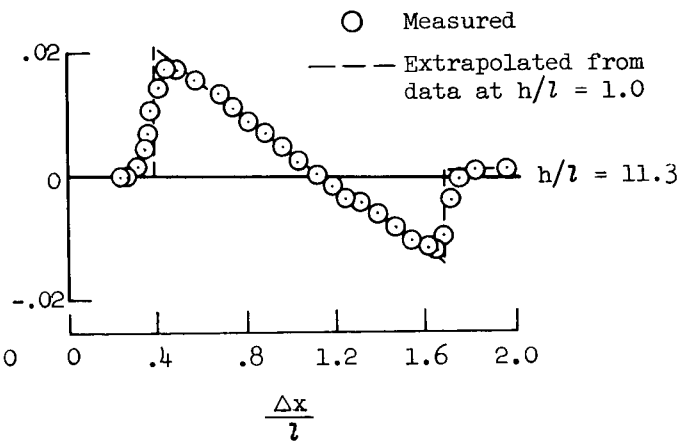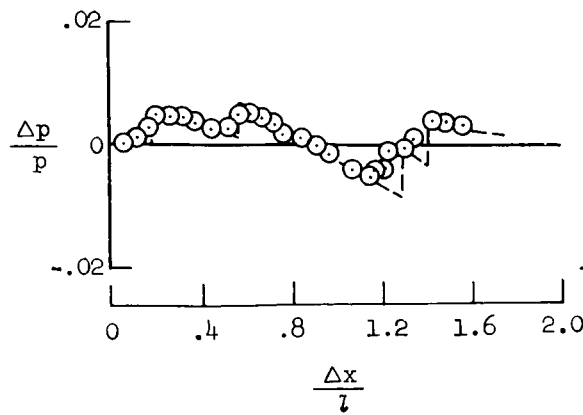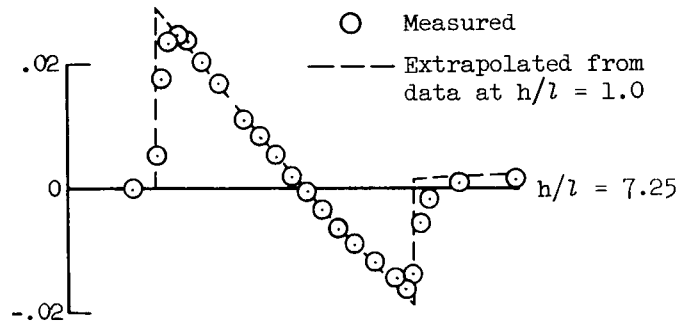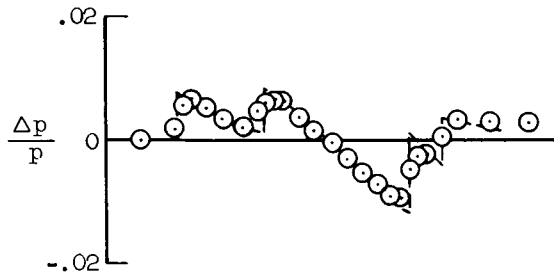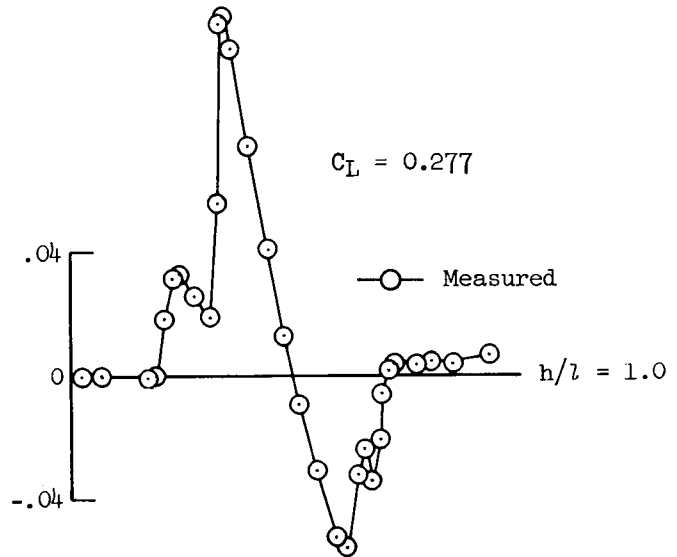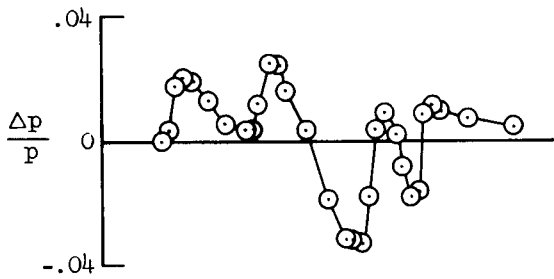
Figure 15.- Flow-field pressures of model IV at two lift coefficients.
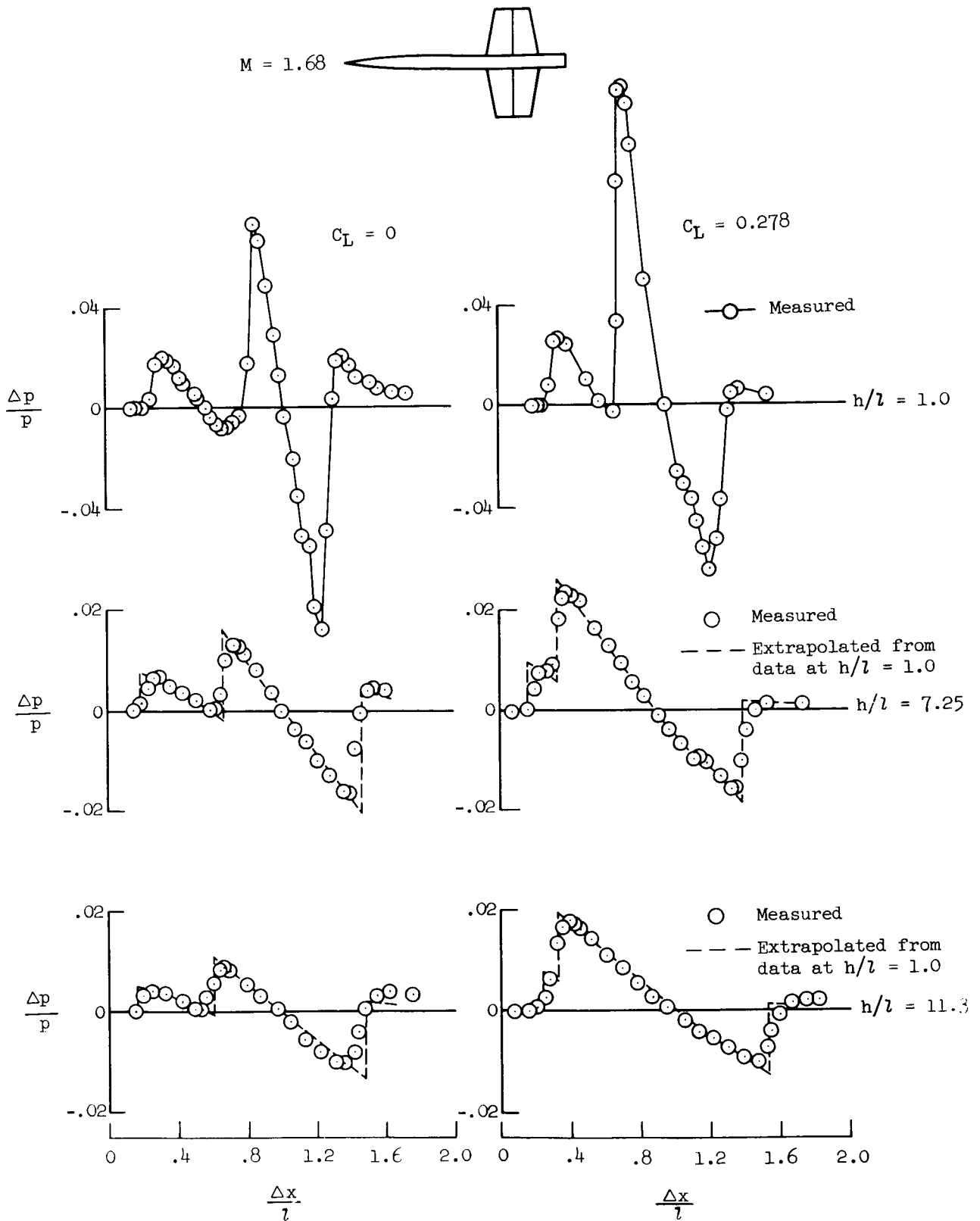
Figure 16.- Flow-field pressures of model V at two lift coefficients.
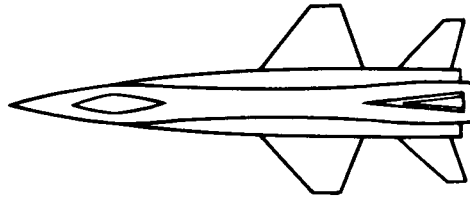
(a) M = 2.0

Figure 17.- Flow-field pressures of model VI at three lift coefficients.
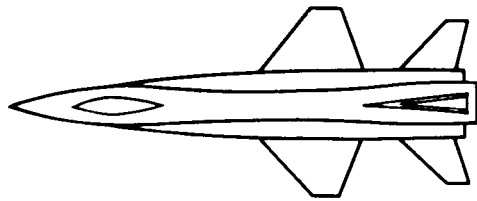
$h/l = 1.50$ $h/l = 3.33$

○ Measured

○ Measured

— — — Extrapolated from data at $h/l = 1.50$

$\frac{\Delta p}{p}$ $C_L = 0$

$\frac{\Delta p}{p}$ $C_L = 0.079$

$\frac{\Delta p}{p}$ $C_L = 0.148$

$\frac{\Delta x}{l}$ $\frac{\Delta x}{l}$
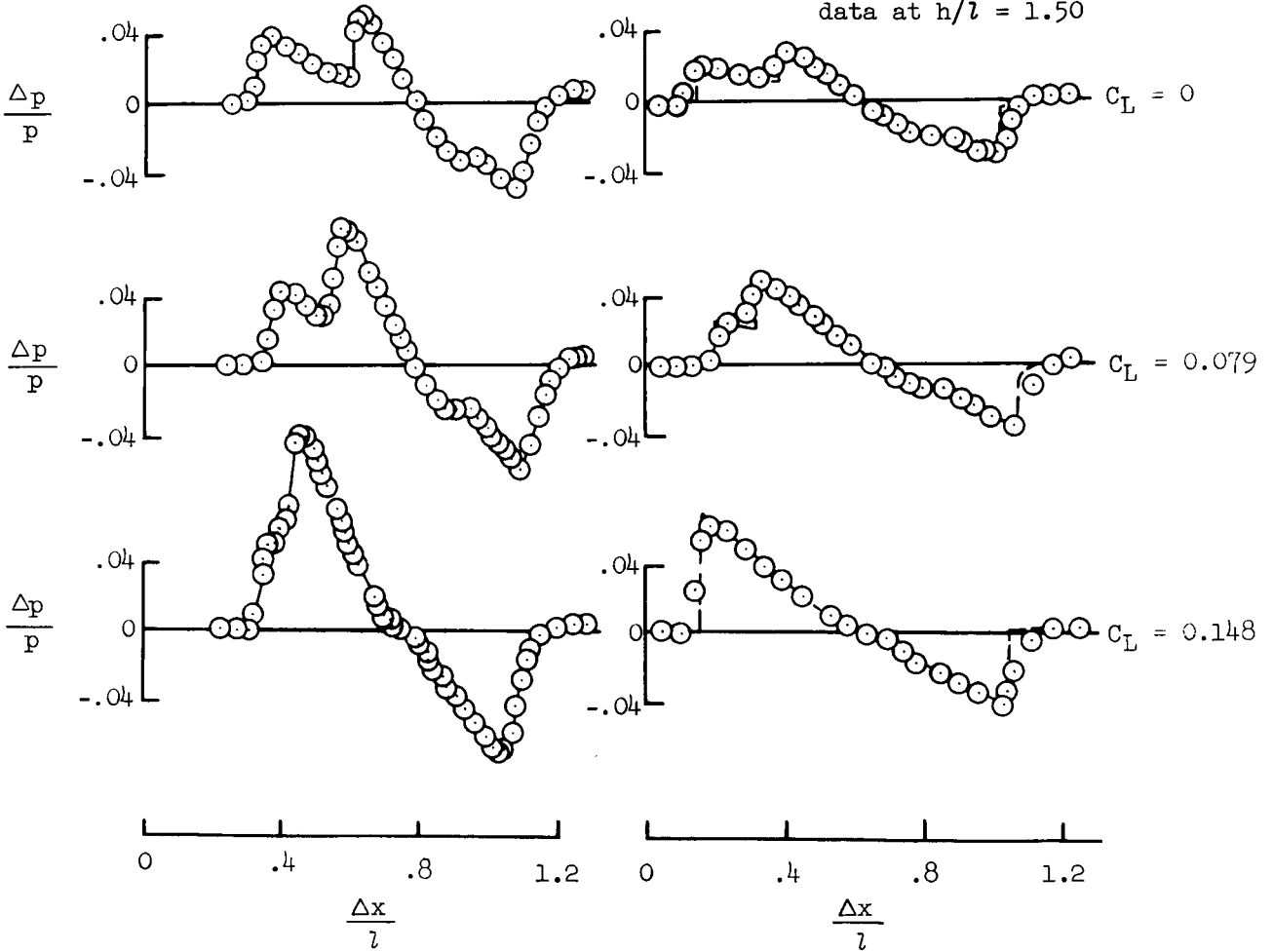
(b) $M = 3.0$

Figure 17.- Concluded.
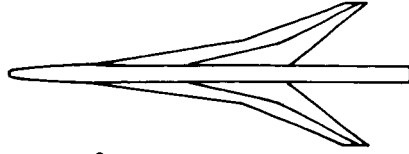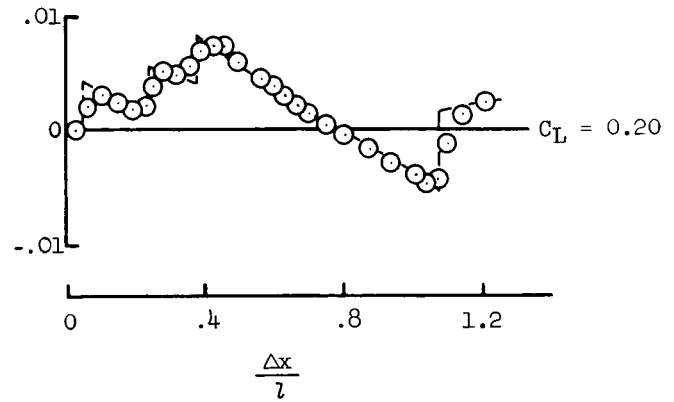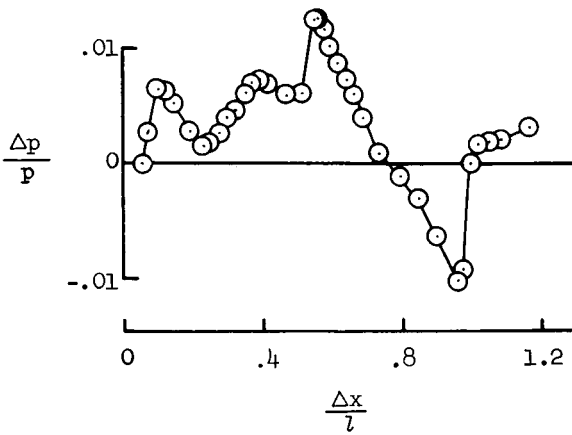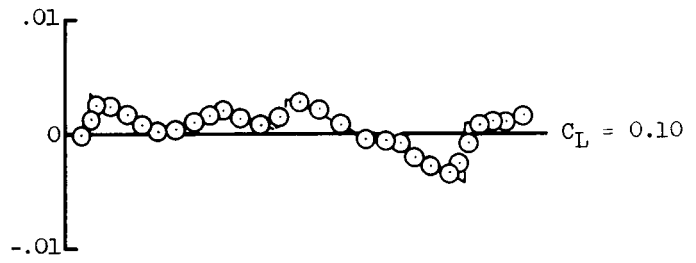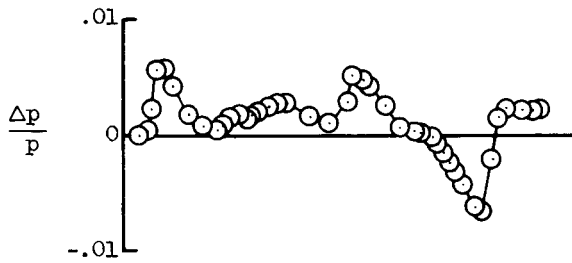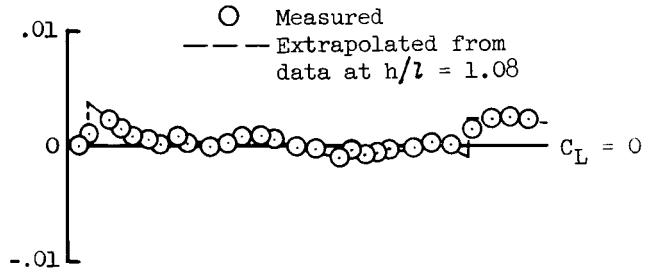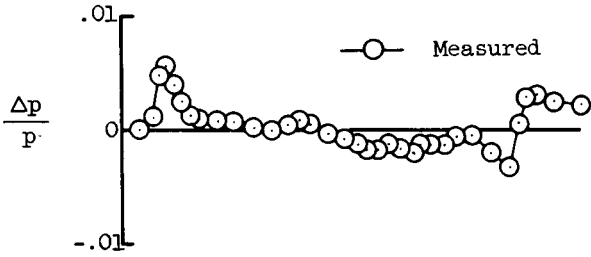
Figure 18.- Flow-field pressures of model VII at three lift coefficients.
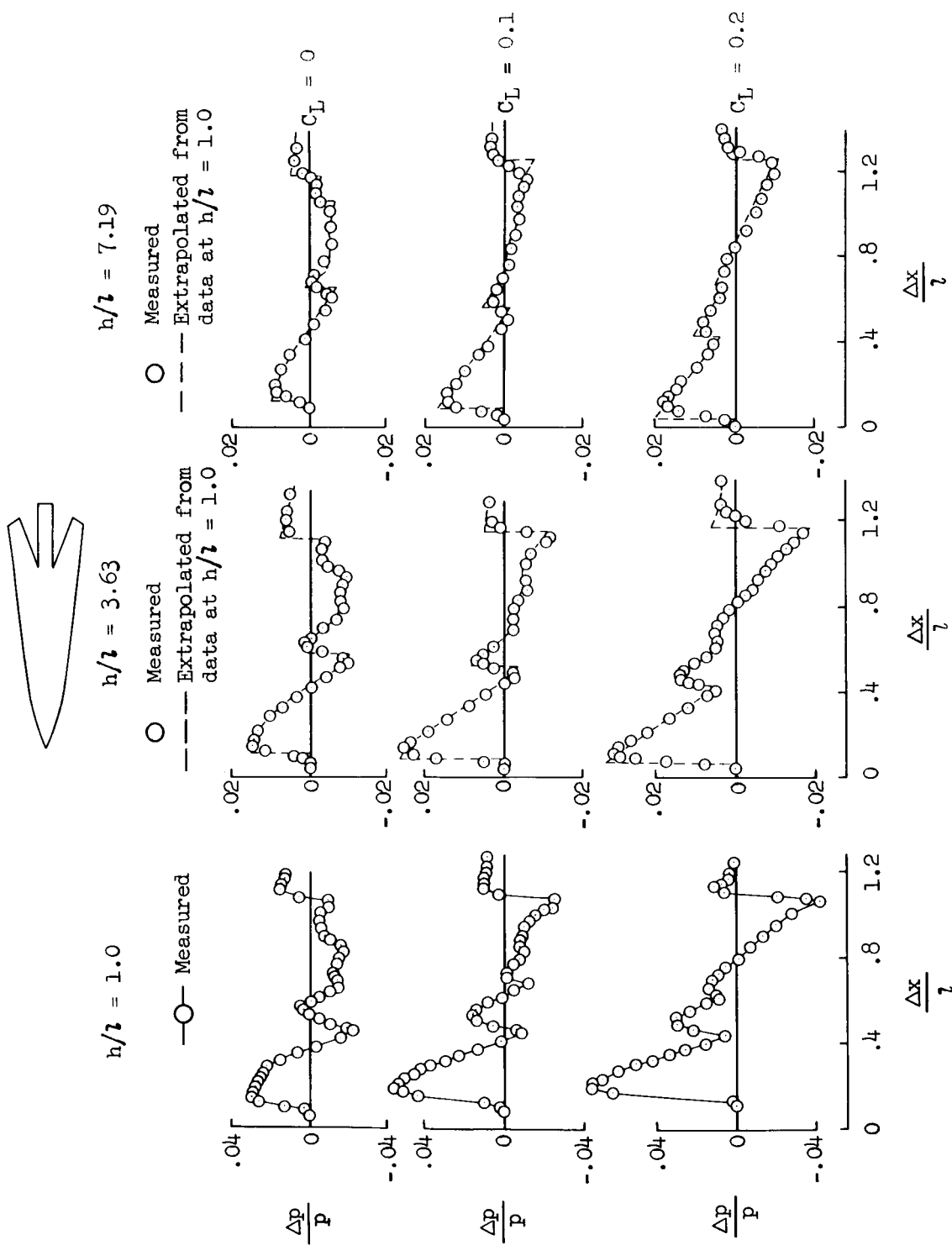
Figure 19.- Flow-field pressures of model VIII at three lift coefficients.

(a) M = 1.68
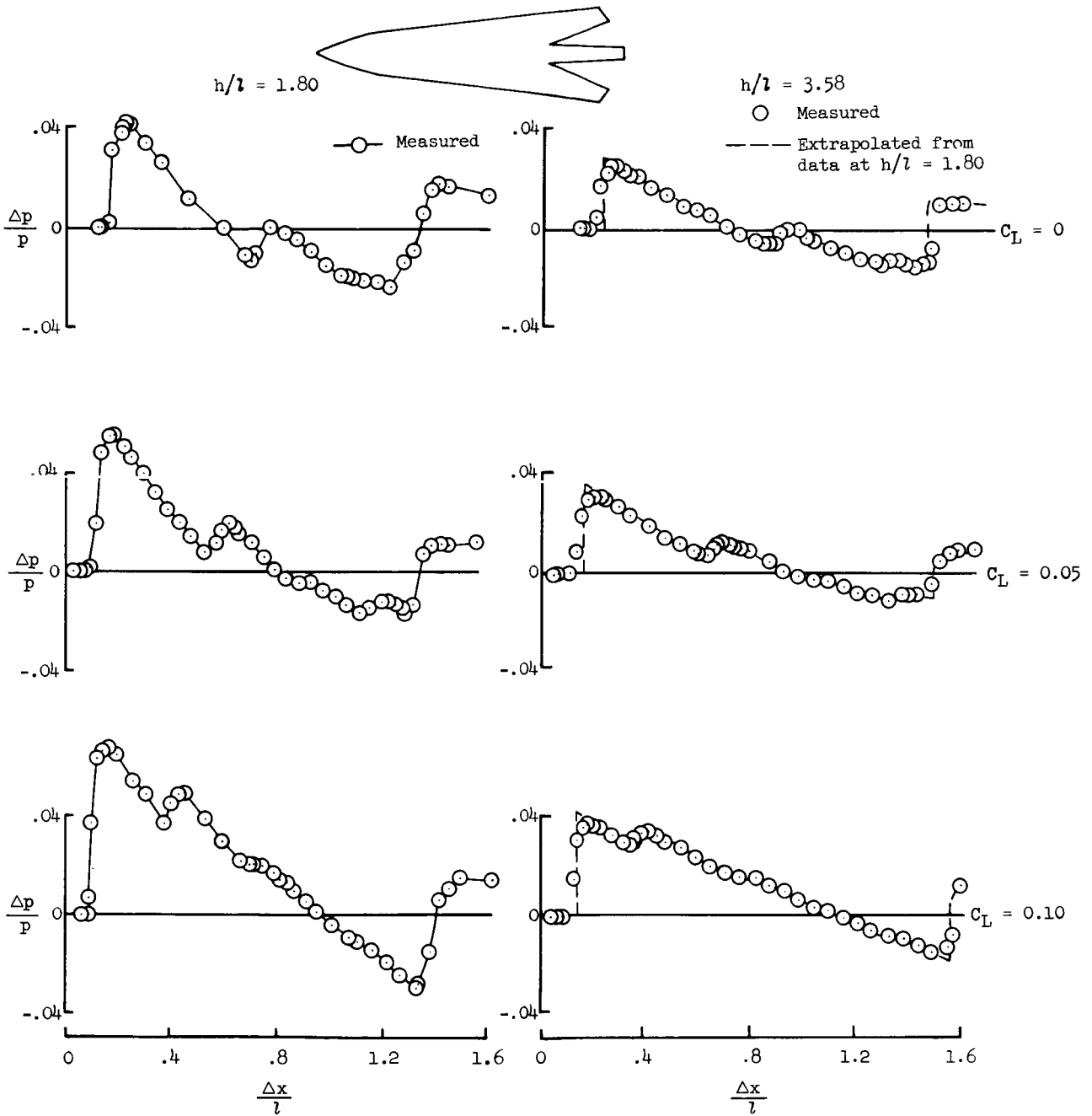
(b) M = 2.70

Figure 19.- Concluded.
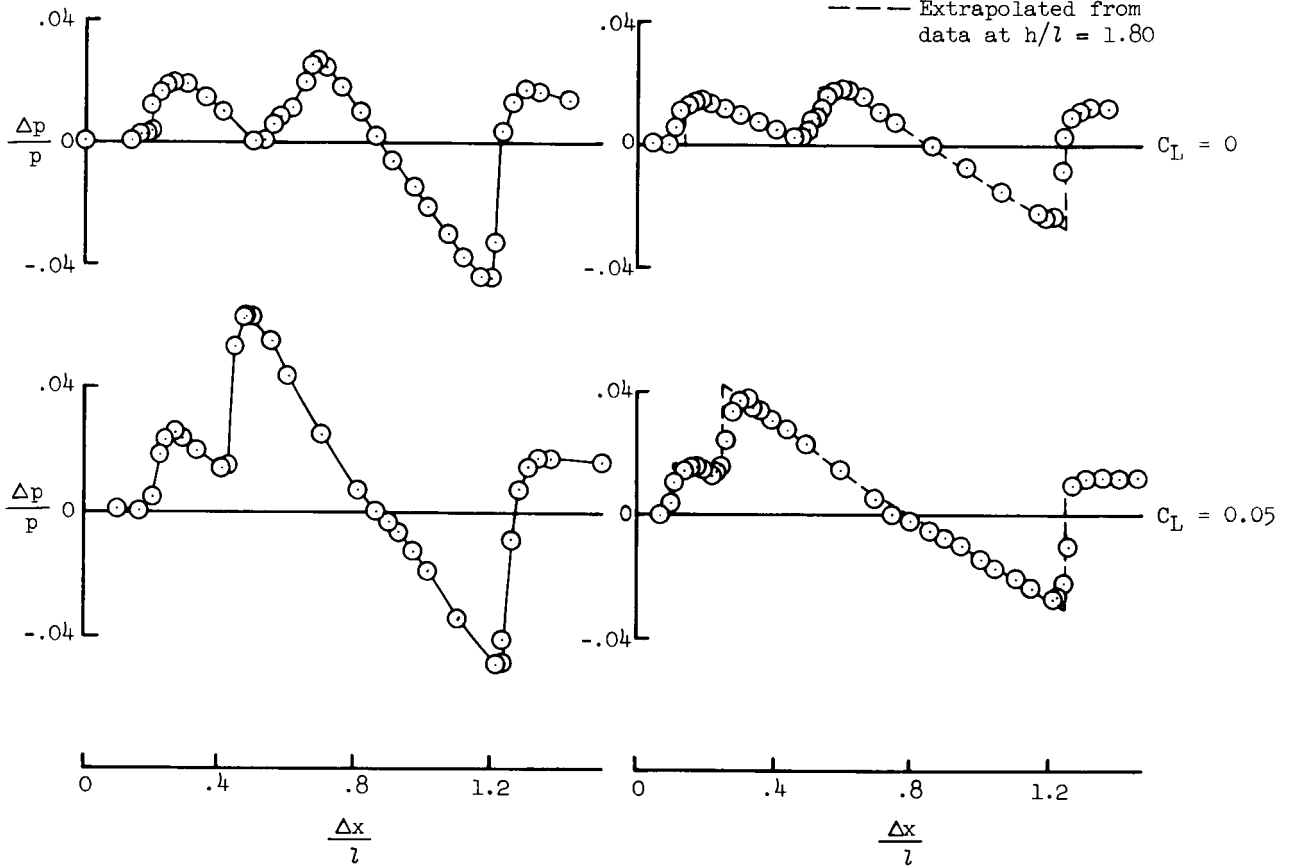
Figure 20.- Flow-field of model IX at two lift coefficients.
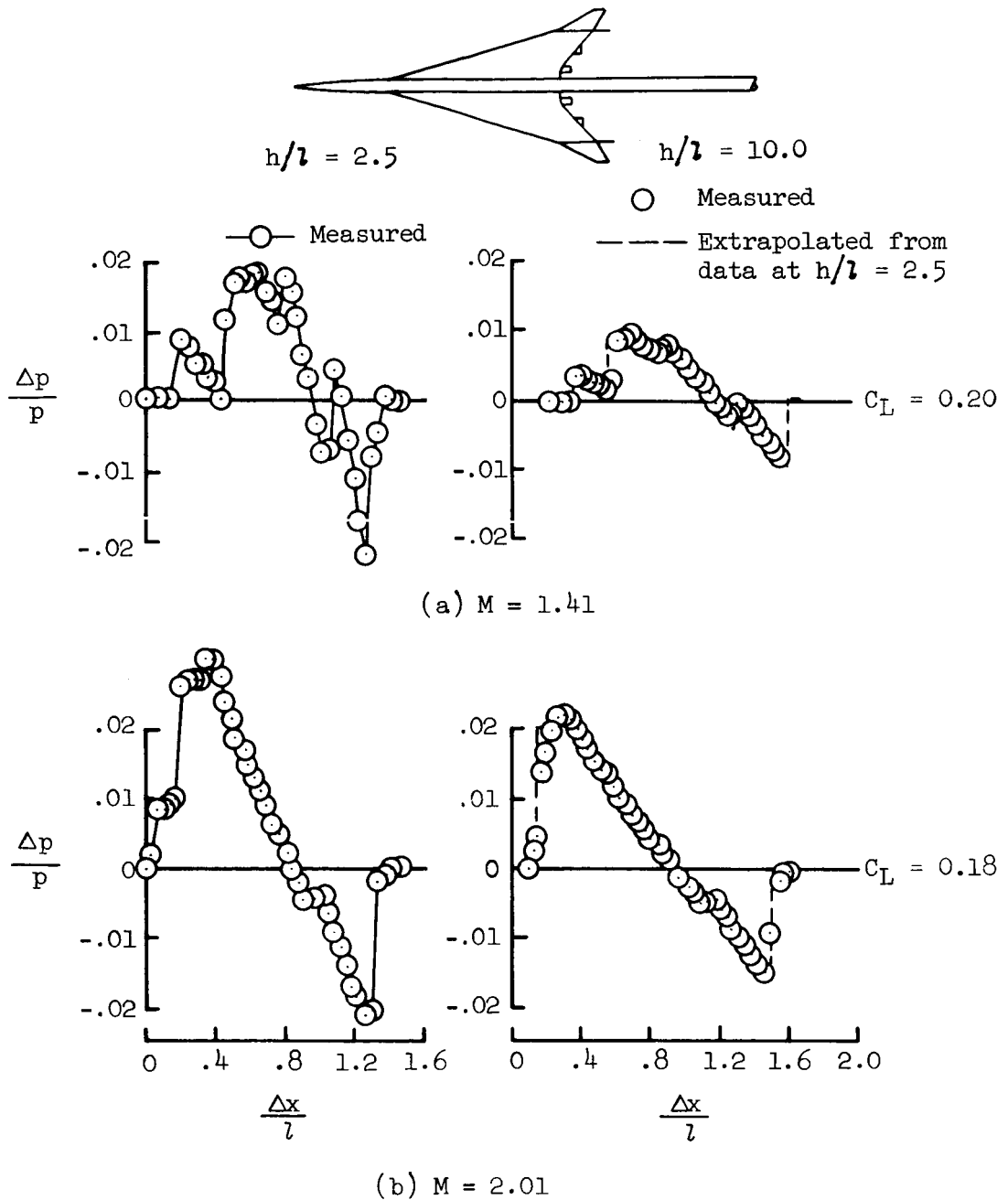
(a) M = 1.41

(b) M = 2.01

Figure 21.- Flow-field pressures of model X (basic model) at two different Mach numbers.
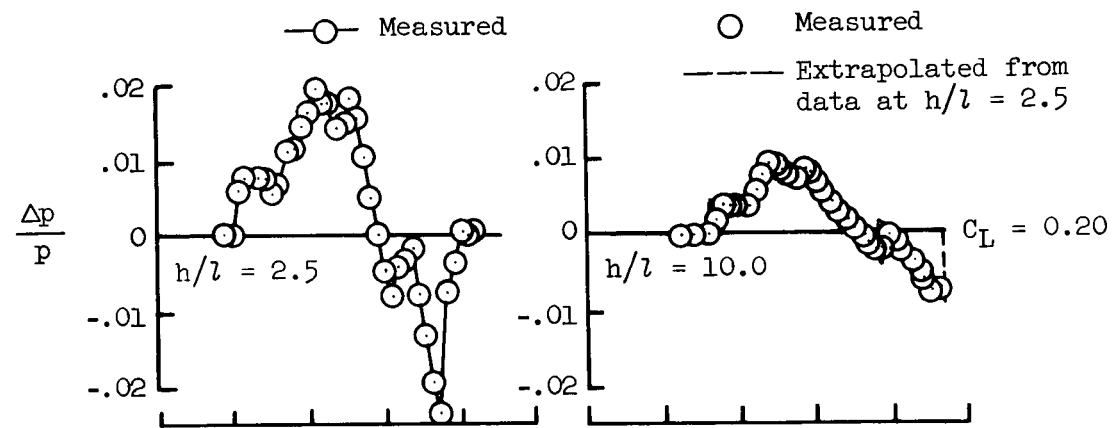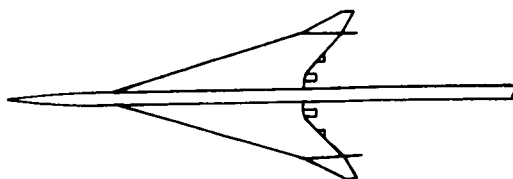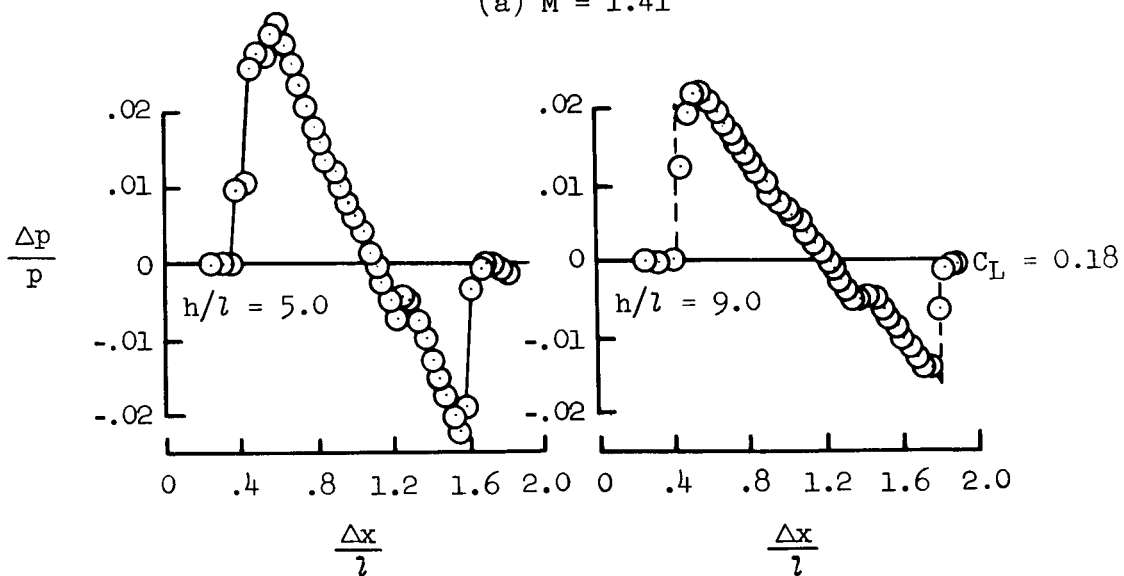
Figure 22.- Flow-field pressures of model XI (modified model).
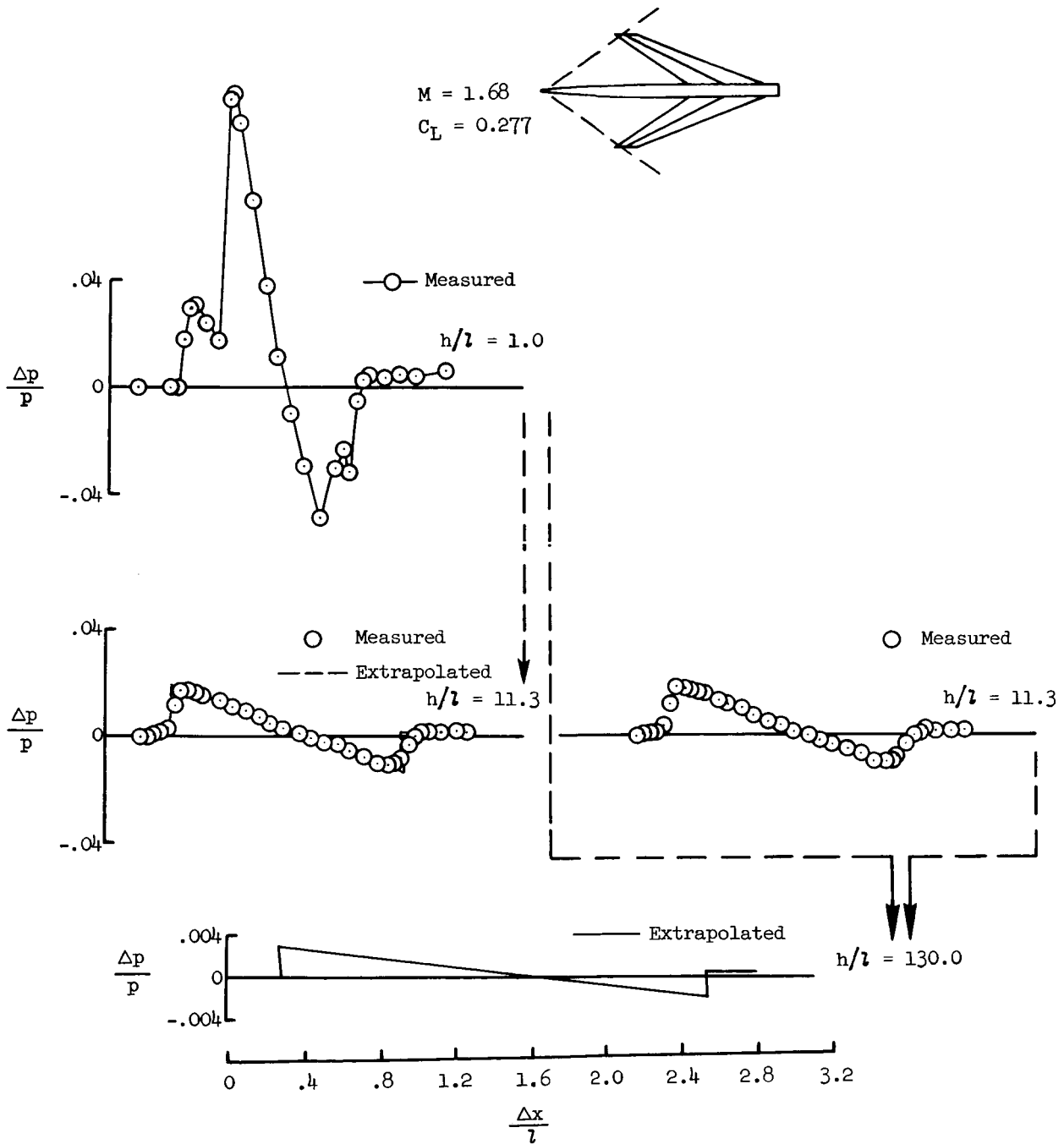
Figure 23.- Pressure signatures of model IV extrapolated to flight altitude.
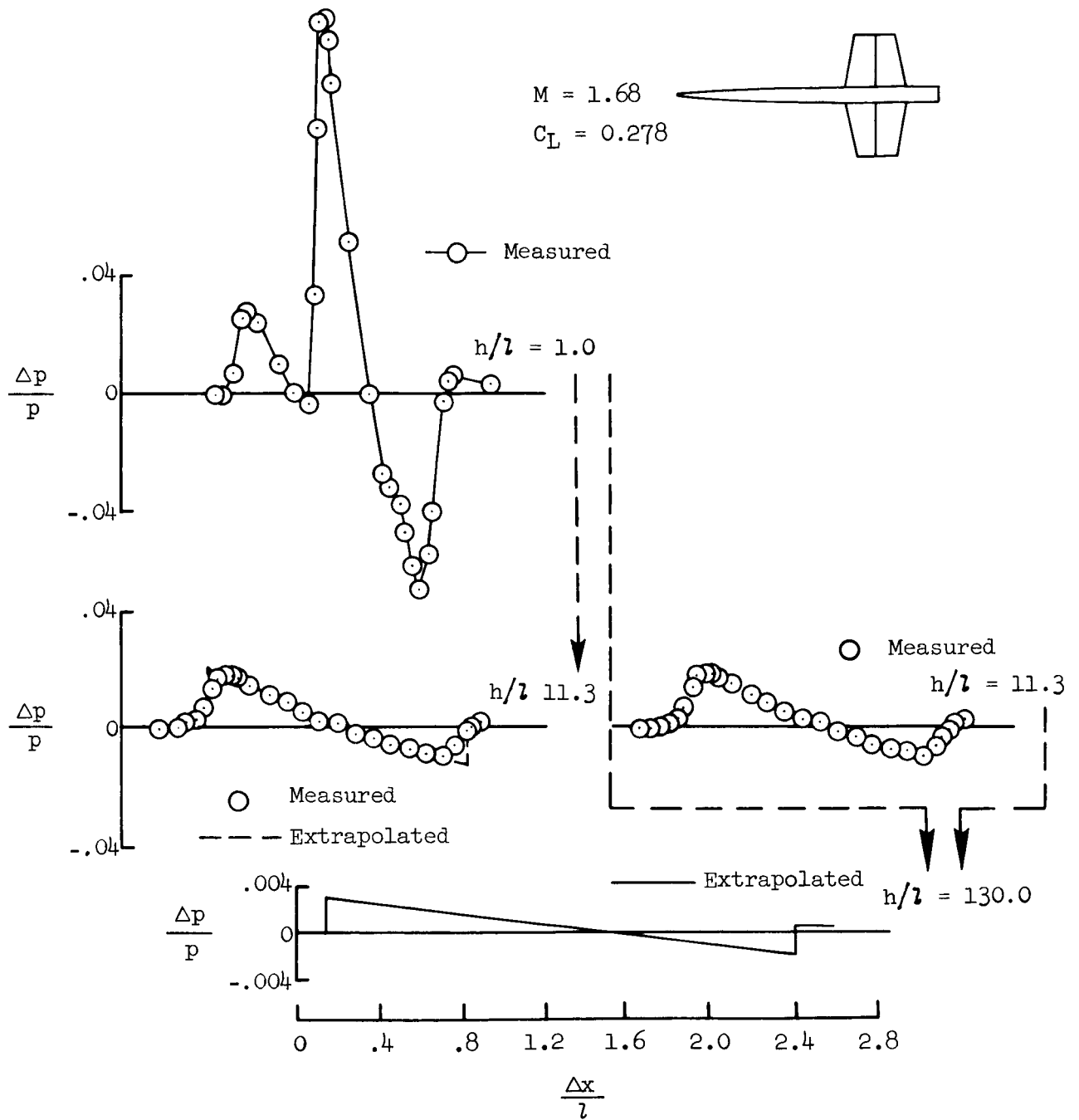
Figure 24.- Pressure signatures of model V extrapolated to flight altitude.